Shape-memory polymers

Shape-memory polymers are an emerging class of active polymers that have dual-shape capability. They can change their shape in a predefined way from shape A to shape B when exposed to an appropriate stimulus. While shape B is given by the initial processing step, shape A is determined by applying a process called programming. We review fundamental aspects of the molecular design of suitable polymer architectures, tailored programming and recovery processes, and the quantification of the shape-memory effect. Shape-memory research was initially founded on the thermally induced dual-shape effect. This concept has been extended to other stimuli by either indirect thermal actuation or direct actuation by addressing stimuli-sensitive groups on the molecular level. Finally, polymers are introduced that can be multifunctional. Besides their dual-shape capability, these active materials are biofunctional or biodegradable. Potential applications for such materials as active medical devices are highlighted.

Marc Behl and Andreas Lendlein*

Center for Biomaterial Development, Institute of Polymer Research, GKSS Research Center Geesthacht, Kantstr. 55, D-14513 Teltow, Germany

**E-mail: andreas.lendlein@gkss.de*

Shape-memory polymers are an emerging class of polymers with applications spanning various areas of everyday life. Such applications can be found in, for example, smart fabrics[1,2], heat-shrinkable tubes for electronics or films for packaging[3], self-deployable sun sails in spacecraft[4], self-disassembling mobile phones[5], intelligent medical devices[6], or implants for minimally invasive surgery[7,8]. These examples cover only a small number of the possible applications of shape-memory technology, which shows potential in numerous other applications. In this review, the fundamental aspects of the shape-memory effect are presented.

Shape-memory polymers are dual-shape materials belonging to the group of 'actively moving' polymers[9]. They can actively change from a shape A to a shape B. Shape A is a temporary shape that is obtained by mechanical deformation and subsequent fixation of that deformation. This process also determines the change of shape shift, resulting in shape B, which is the permanent shape. In shape-memory polymers

ISSN:1369 7021 © Elsevier Ltd 2007

reported so far, heat or light has been used as the stimulus. Using irradiation with infrared light, application of electric fields, alternating magnetic fields, or immersion in water, indirect actuation of the shape-memory effect has also been realized. The shape-memory effect only relies on the molecular architecture and does not require a specific chemical structure in the repeating units. Therefore, intrinsic material properties, e.g. mechanical properties, can be adjusted to the need of specific applications by variation of molecular parameters, such as the type of monomer or the comonomer ratio.

General concept of shape-memory polymers

The shape-memory effect is not an intrinsic property, meaning that polymers do not display this effect by themselves. Shape memory results from a combination of polymer morphology and specific processing and can be understood as a polymer functionalization. By conventional processing, e.g. extruding or injection molding, the polymer is formed into its initial, permanent shape B. Afterwards, in a process called programming, the polymer sample is deformed and fixed into the temporary shape A. Upon application of an external stimulus, the polymer recovers its initial permanent shape B. This cycle of programming and recovery can be repeated several times, with different temporary shapes in subsequent cycles. In comparison with metallic shape-memory alloys, this cycle of programming and recovery can take place in a much shorter time interval and polymers allow a much higher deformation rate between shapes A and B[10].

Shape-memory polymers are elastic polymer networks that are equipped with suitable stimuli-sensitive switches[11,12]. The polymer network consists of molecular switches and netpoints (Fig. 1). The netpoints determine the permanent shape of the polymer network and can be of a chemical (covalent bonds) or physical (intermolecular interactions) nature. Physical cross-linking is obtained in a polymer whose morphology consists of at least two segregated domains, as found for example in block copolymers. Here, domains related to the highest thermal transition temperature (T_{perm}) act as netpoints (a hard segment), while chain segments in domains with the second highest thermal transition T_{trans} act as molecular switches (a switching segment). If the working temperature is higher than T_{trans}, then the switching domains are flexible, resulting in an entropic elastic behavior of the polymer network above T_{trans}. If the sample has been previously deformed by application of an external stress, it snaps back into its initial shape once the external stress is released. The molecular mechanism of the shape-memory effect is illustrated for the thermally induced shape-memory effect in Fig. 1. The shape-memory polymer network consists of covalent netpoints and switching segments based on a physical interaction.

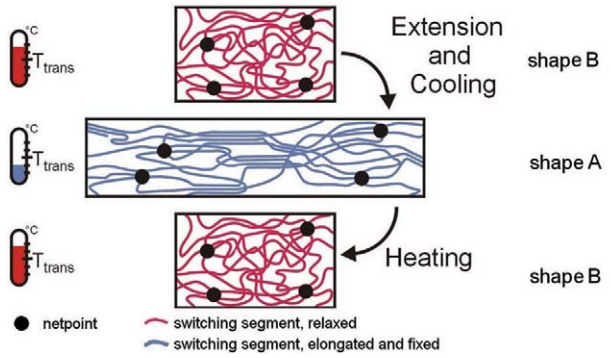

Fig. 1 Molecular mechanism of the thermally induced shape-memory effect T_{trans} = thermal transition temperature related to the switching phase. (Adapted with permission from[11]. © 2002 Wiley-VCH.)

To display shape-memory functionality, the polymer network has to be temporarily fixed in a deformed state under environmental conditions relevant to the particular application. This requires the deformed chain segments, which are under external stress, to be reversibly prevented from recoiling, and is achieved by the introduction of reversible netpoints as the molecular switches. These additional netpoints can be formed by physical interactions or by covalent bonds. Physical cross-linking is obtained by vitrification or crystallization of domains related to T_{trans}. These switching domains can be formed either by the chain segments driving the entropic elastic behavior themselves or by side chains, whose aggregation is able temporarily to prevent recoiling of that chain's side chains or the side chain segments themselves. Reversible covalent cross-linking is obtained by attaching functional groups to the chain segments. Controlled by an external stimulus, these functional groups must be able to form covalent bonds reversibly by reaction with each other or suitable counterpart functional groups.

Most of the shape-memory polymers reported so far use heat as a stimulus. Here, the stimulation results from thermally induced cleavage of the additional cross-links. If these additional cross-links are based on physical interactions, a further distinction in T_{trans} can be made, which can be either a glass transition T_g or a melting temperature T_m. While glass transitions can extend over a broad temperature interval, melting occurs over a relatively small temperature range. If the cross-links are functional groups able to undergo photoreversible reactions, the shape-memory technology is extended to use light as a stimulus. Other stimuli like electrical currents or electromagnetic fields can be used to heat the material indirectly.

Shape-memory properties are quantified in cyclic mechanical tests for the different stimuli[11-13]. As most stimuli are based on heat or light, thermo- or photomechanical test procedures have been developed. In these cyclic tests, the strain fixity rate R_f, the strain recovery rate R_r, and, in the case of thermal stimulation, the switching temperature T_{switch} are determined. For each number of cycles (N), R_f quantifies the ability to fix a mechanical deformation ε_m, resulting in a temporary shape $\varepsilon_u(N)$. R_r quantifies the ability to restore the mechanical deformation of the permanent shape $\varepsilon_p(N)$ after application of a certain deformation ε_m, as it builds the ratio between the change in strain recorded during shape-memory effect $\varepsilon_m - \varepsilon_p(N)$ and the change

in strain in the course of programming given by $\varepsilon_m - \varepsilon_p(N-1)$. From the equations given below (eqs 1 and 2), it is obvious that ideally R_f and R_r should be 100%:

$$R_f(N) = \frac{\varepsilon_u(N)}{\varepsilon_m} \quad (1)$$

$$R_r(N) = \frac{\varepsilon_m - \varepsilon_p(N)}{\varepsilon_m - \varepsilon_p(N-1)} \quad (2)$$

In a typical stress-controlled programming cycle (Fig. 2), the test specimen is clamped into the tensile tester, the sample is elongated to ε_m while the molecular switches are open (step 1). Opening of the molecular switches is realized in thermally induced shape-memory materials by heating to a temperature T_{high} above T_{trans}, and in light-induced shape-memory materials by irradiation of suitable wavelengths λ_1 to cleave photosensitive bonds. This strain is maintained for some time to allow relaxation of the polymer chains and afterwards the experiment is continued in a stress-controlled mode. While being held under constant stress σ_m, this temporary shape is fixed by closing of the molecular switches (step 2). Closing of the switches occurs in thermally induced shape-memory materials by controlled cooling to a temperature below T_{trans} or in light-induced shape-memory materials by irradiation with other suitable wavelengths λ_2. Afterwards, the strain is reduced until a stress-free condition is achieved at 0 MPa (step 3). Finally, the molecular switches are opened again, while the tensile stress is held constant at 0 MPa, resulting in the contraction of the test specimen and resumption of its permanent shape (step 4).

Several models for the prediction of shape-memory effects have been described[14-17]. They are all based on uniaxial deformation processes but differ in their modeling approach. These approaches

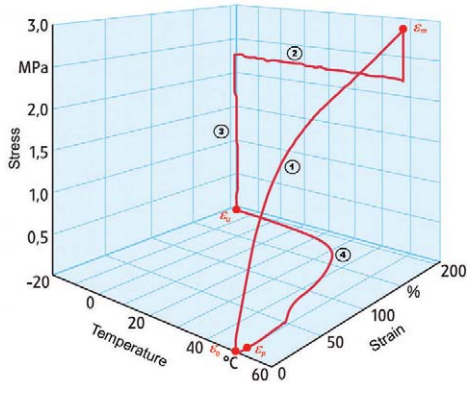

Fig. 2 Typical stress-strain-temperature diagram (first cycle) for a thermoplastic shape-memory polymer with a thermally induced shape-memory effect[7,81]. Step 1 of the experiment is strain controlled, while steps 2 through 4, to the beginning of the next cycle are stress-controlled. (Reprinted with permission from[81]. © 2006 Hanser Publishing Company.)

are based either on a mechanical modeling approach[14,17] or a thermodynamic approach[15,16]. They allow the prediction of irrecoverable strain[14,16], temperature-dependent stress and strain[15], or stress and strain[17] for polymers under deformation.

Thermally induced shape-memory effect

Examples of thermally induced shape-memory polymers

An important group of physically cross-linked shape-memory polymers are linear block copolymers. Block copolymers with $T_{trans} = T_m$ are reviewed elsewhere[11], and include polyurethanes and polyetheresters. In polyesterurethanes, the urethane segments act as hard segments, while poly(ε-caprolactone) (T_m = 44-55°C) forms the switching segment[18-20]. Additionally, polyesterurethanes containing mesogenic moieties have been reported[21,22]. In block copolymers with *trans*-(polyisoprene) switching segments and urethane hard segments, the microphase separation has been investigated[23]. Here, the polyurethane segments act as physical cross-links and assemble into spherical domains. T_{trans} is based on a melting transition of the *trans*-(polyisoprene) switching segments.

In block copolymers, the shape-memory effect can also be based on a glass transition temperature ($T_{trans} = T_g$). A typical example is polyurethanes, whose switching domains are, in most cases, mixed phases[24].

Another class of thermoplastic shape-memory polymers with $T_{trans} = T_g$ are polyesters. In copolyesters based on poly(ε-caprolactone) and poly(butylene terephthalate), the poly(butylene terephthalate) segments act as physical cross-linkers[25]. The shape-memory capability can also be added to a polymer using a polymer analogous reaction. A polymer analogous reaction is the application of a standard organic reaction (like the reduction of a ketone to an alcohol) to a polymer having several of these reactive groups. An example is the polymer analogous reduction of a polyketone with $NaBH_4$/THF, which results in a poly(ketone-*co*-alcohol)[26]. The polyketones are synthesized by late transition metal catalyzed polymerization of propene, hex-1-ene, or a mixture of propene and hex-1-ene with CO. The T_g of this polymer is directly related to the degree of reduction, which can be adjusted by the amount of $NaBH_4$/THF. The most promising shape-memory material is a partly reduced poly(ethylene-*co*-propene-*co*-carbonoxide), which displayed a phase-separated morphology with hard microcrystalline ethylene/CO-rich segments within a softer amorphous polyketone ethylene-propene/CO-rich matrix. The crystalline domains of this material work as physical cross-linkers. This results in an elastic behavior above T_g, because the glass transition temperature ($T_{trans} = T_g$) is related to the switching phase. Partial reduction of the material allows control of T_g, which can be adjusted from below room temperature to 75°C.

Covalently cross-linked polymers can be obtained by cross-linking during synthesis or postpolymerization, which involves radiation and chemical methods. As an example, dual-shape capability can be added

to polyethylene[3] and its copolymers[27,28] by cross-linking with ionizing radiation (γ-radiation, neutrons). Radiation cross-linking of poly(ε-caprolactone) results in mainly molecular chain scission and loss of useful mechanical properties[29]. By blending poly(ε-caprolactone) with polymethylvinylsiloxane, radiation cross-linking of the blend can be achieved and shape-memory properties can be added to the material[30]. Another option is the chemical cross-linking of poly[ethylene-*co*-(vinylacetate)] with dicumylperoxide as a radical initiator[31]. The same radical initiator has been used for the cross-linking of semicrystalline polycyclooctene[32]. In Fig. 3, a material based on a postpolymerized poly(ε-caprolactone)dimethacrylate is shown as an example of a thermally induced shape-memory effect. A covalently cross-linked polymer from a natural source has been prepared by cationic polymerization of soybean oil with styrene and divinylbenzene, using norbornadiene or dicyclopentadiene as a cross-linker[33]. A material consisting of 45 wt.% soybean oil, 27 wt.% styrene, and 17 wt.% divinylbenzene (and 5 wt.% Norway pronova fishoil and 3 wt.% boron trifluoride diethyl etherate) displays 97% strain fixity and 100% shape recovery in bending tests.

Synthesis of covalently cross-linked polymer networks during polymerization can be realized by (co)condensation or poly-(co)condensation of one or several monomers, where at least one is trifunctional, or by copolymerization of monofunctional monomers with low molecular weight or oligomeric cross-linkers. An example of the latter is a copolymer of stearyl acrylate, methacrylate, and *N,N*-methylenebisacrylamide as the cross-linker[34]. Here, crystalline domains of stearyl side chains form the switching phase. In multiphase copolymer networks obtained by the radical polymerization or copolymerization of poly(octadecyl vinyl ether)diacrylates or -dimethacrylates with butyl acrylate as the comonomer, the situation is similar[35,36]. In both cases, the crystalline domains of octadecyl side chains again act as switching segments.

An example of a cross-linked polymer network synthesized by polyaddition of monofunctional monomers with low molecular weight or oligomeric cross-linkers has been realized in polyurethanes by the addition of trimethylol to the reaction mixture[37].

Reaction of tetrafunctional silanes, working as netpoints, with oligomeric silanes, which work as spacers and to which two distinct benzoate-based mesogenic groups have been attached, results in formation of a main-chain smectic-C elastomer[38]. In contrast to other liquid-crystalline elastomers, which display a shape-changing behavior and have been compared to shape-memory polymers recently[9], these elastomers have shape-memory properties. The cross-link process during synthesis defines the permanent shape. The shape-memory effect is triggered by the thermal transition of the liquid-crystalline domains. In the programming process, the polymer network is heated to the isotropic state of the liquid-crystalline domains, stretched or twisted, and then cooled below the clearing transition temperature of the smectic-C mesogens. Upon reheating over this clearing transition, the permanent shape can be recovered. In contrast to shape-changing liquid-crystalline elastomer systems, these polymers display shape-memory behavior because the liquid-crystalline moieties work as a switch. In shape-changing liquid-crystalline elastomers, the molecular movement of the single liquid crystals is converted into a macroscopic movement.

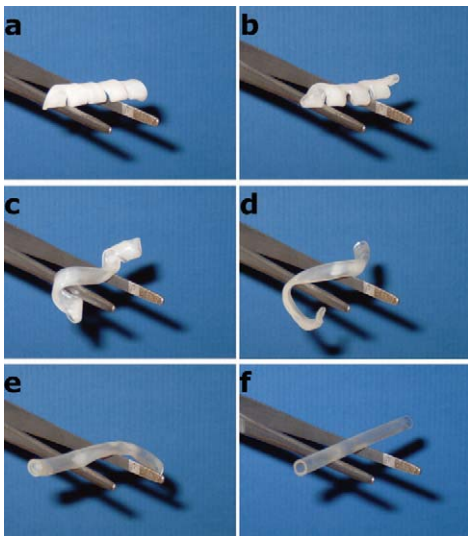

Fig. 3 Time series photographs that show the recovery of a shape-memory tube. (a)-(f) Start to finish of the process takes a total of 10 s at 50°C. The tube was made of a poly(ε-caprolactone)dimethacrylate polymer network (the M_n of the network's switching segments was 10^4 gmol^{-1}) that had been programmed to form a flat helix. (Reprinted with permission from[59]. © 2004 Nature Publishing Group.)

Indirect actuation of the thermally induced shape-memory effect

Indirect actuation of the shape-memory effect has been realized by two different strategies. One method involves indirect heating, e.g. by irradiation. The other possibility is to lower T_{trans} by diffusion of low molecular weight molecules into the polymer, which works as a plasticizer. This allows the triggering of the shape-memory effect while the sample temperature remains constant.

Instead of increasing the environmental temperature, thermally induced shape-memory polymers can be heated by illumination with infrared light. This concept has been demonstrated in a laser-activated polyurethane medical device[39,40]. In such devices, heat transfer can be enhanced by incorporation of conductive fillers, such as conductive ceramics, carbon black, and carbon nanotubes (Fig. 4)[41-43]. This incorporation of particles also influences the mechanical properties: incorporation of microscale particles results in increased stiffness and recoverable strain levels[44,45], and can be further enhanced by the incorporation of nanoscale particles[46,47]. To achieve an enhanced photothermal effect, the molecular structure of the particles has to be considered. Polyesterurethanes reinforced with carbon nanotubes

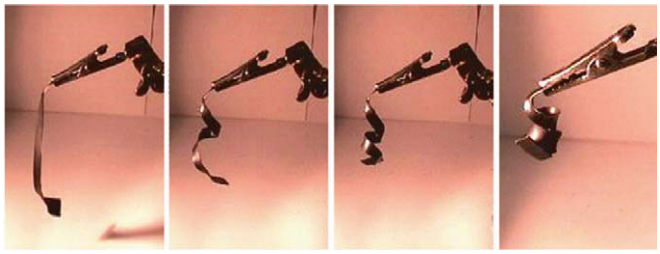

Fig. 4 Strain recovery under infrared radiation (exposure from the left). Infrared absorption, nonradiative energy decay, and resulting local heating is constrained to the near-surface region of a stretched ribbon, resulting in strain recovery of the near-surface region and curling of the ribbon toward the infrared source within 5 s. (Reprinted with permission from[48]. © 2004 Nature Publishing Group.)

or carbon black of similar size display increased strain and fixity[48]. While carbon-black-reinforced materials show limited shape recovery of around 25-30%, in carbon-nanotube-reinforced polymers, an R_r of almost 100% can be observed and has been attributed to a synergy between the anisotropic carbon nanotubes and the crystallizing polyurethane switching segments.

A certain level of conductivity can be reached by incorporating carbon nanotubes into shape-memory polyurethanes[49]. Upon application of an electrical current, the sample temperature is increased as a result of the high ohmic resistance of the composite. This effect has been used to trigger the shape-memory effect.

Incorporation of magnetic nanoparticles consisting of Fe(III)oxide cores in a silica matrix into shape-memory thermoplastics enables remote actuation of the thermally induced shape-memory effect using magnetic fields (Fig. 5)[50]. Here, the sample temperature is increased by inductive heating of the nanoparticles in an alternating magnetic field (f = 258 kHz, H = 7-30 kAm^{-1}). Two different thermoplastic materials have been used as the matrix. The first material was an aliphatic polyetherurethane (TFX) from methylene bis(p-cyclohexyl isocyanate), butanediol, and polytetrahydrofuran, while the other was a biodegradable multiblock copolymer (PDC) with poly(p-dioxanone) as the hard segment and poly(ε-caprolactone) as the switching segment. While TFX has an amorphous switching phase, PDC has a crystallizable switching segment. Indirect magnetic actuation has also been realized

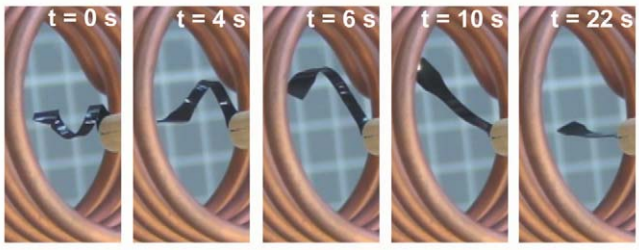

Fig. 5 Magnetically induced shape-memory effect of a thermoplastic composite consisting of Fe(III)oxide nanoparticles in a silica matrix and polyetherurethane. (Reprinted with permission from[50]. © 2006 National Academy of Sciences.)

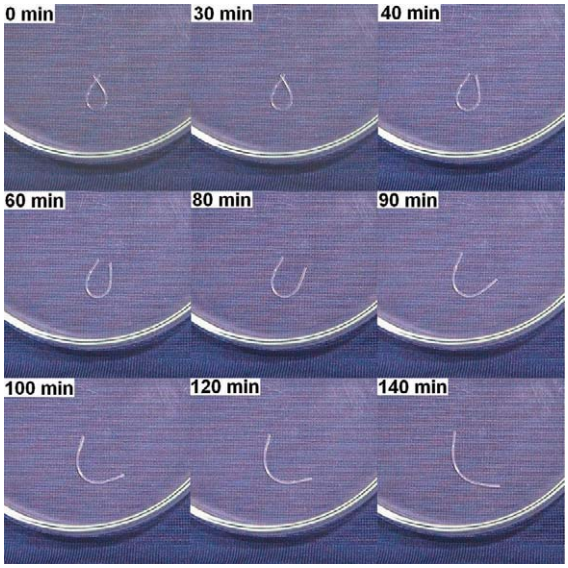

Fig. 6 Water-driven actuation of a shape-memory effect. A shape-memory polyurethane with a circular temporary shape is immersed into water. After 30 min, the recovery of the linear permanent shape begins. (Reprinted with permission from[53]. © 2005 American Institute of Physics.)

by the incorporation of Ni-Zn ferrite particles into a commercial ester-based thermoset polyurethane[51].

Indirect actuation of the shape-memory effect by lowering T_{trans} has been shown for commercially available polyurethanes[52-54] and its composites with carbon nanotubes[55]. In all cases, the temporary shape is programmed by conventional methods for thermally induced shape-memory polymers. When immersed in water, moisture diffuses into the polymer sample and acts as a plasticizer, resulting in shape recovery (Fig. 6). In the polymers and composites based on polyurethanes, T_g is lowered from 35°C to below ambient temperature. It can be shown that the lowering of T_g depends on the moisture uptake, which in turn depends on the immersion time. In time-dependent immersion studies, it has been shown that the water uptake can be adjusted between 0-4.5 wt.%, which goes along with a lowering of T_g of between 0 K and 35 K. As the maximum moisture uptake achieved after 240 hours was around 4.5 wt.%, this shape-memory polymer still has to be understood as a polymer and not as a hydrogel. A different strategy for water-actuated shape-memory polymers has been realized in polyetherurethane polysilesquisiloxane block copolymers[56]. Here, low molecular weight poly(ethylene glycol), or PEG, has been used as the polyether segment. Upon immersion in water, the PEG segment dissolves, resulting in the disappearance of T_m and recovery of the permanent shape.

Light-induced shape-memory effect

Light-induced stimulation of shape-memory polymers has been realized through the incorporation of reversible photoreactive molecular switches[13,57,58]. This stimulation is independent of any temperature

effects and must be differentiated from the indirect actuation of the thermally induced shape-memory effect.

To introduce light sensitivity into shape-memory polymers, cinnamic acid (CA) or cinnamylidene acetic acid (CAA) moieties, which work as light-triggered switches, have been incorporated into the polymer architecture (Fig. 7)[57]. Upon irradiation with light of suitable wavelength, a [2 + 2] cycloaddition reaction occurs between two of these light-sensitive moieties, forming a cyclobutane-ring and in this way covalent cross-links. Irradiation with a different wavelength results in cleavage of the newly formed bonds.

Two alternative strategies have been used in designing the molecular structure of light sensitive-polymers: a graft polymer and an interpenetrating polymer. In the graft polymer, CA molecules are grafted onto a permanent polymer network created by the copolymerization of n-butylacrylate, hydroxyethyl methacrylate, ethylenegylcol-1-acrylate-2-CA, and poly(propylene glycol)-dimethacrylate) (M_n = 560 gmol^{-1}) as the cross-linker. Loading a permanent polymer network, made from butylacrylate and 3 wt.% poly(propylene glycol)-dimethylacrylate (M_n = 1000 gmol^{-1}) as a cross-linker, with 20 wt.% star-poly(ethylene glycol) end capped with terminal CAA groups yields a photosensitive interpenetrating network. In both cases, the permanent shape is determined by the cross-links of an amorphous polymer network. In the programming cycle, the polymer is first stretched, resulting in strained, coiled polymer segments. Afterwards, the network is irradiated with ultraviolet (UV) light with a wavelength > 260 nm, creating new covalent netpoints that fix the strained form in a temporary shape. The permanent shape is recovered upon irradiation with UV light of λ < 260 nm through cleavage of the cross-links.

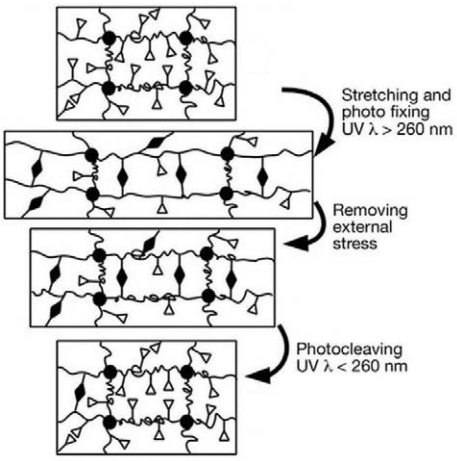

Fig. 7 Molecular mechanism responsible for the light-induced shape-memory effect in a grafted polymer network. Chromophores (open triangles) are grafted onto the permanent polymer network (filled circles, permanent cross-links). Photoreversible cross-links (filled diamonds) are formed during fixation of the temporary shape by ultraviolet (UV) light irradiation of a suitable wavelength. Recovery is realized by UV irradiation at a second wavelength. (Reprinted with permission from[57]. © 2005 Nature Publishing Group.)

Biomedical applications of shape-memory polymers

An attractive application area for shape-memory polymers is their use in active medical devices[59,60]. First examples include a laser-activated device for the mechanical removal of blood clots (Fig. 8)[39,40]. The device is inserted by minimally invasive surgery into the blood vessel and, upon laser activation, the shape-memory material coils into its permanent shape, enabling the mechanical removal of the thrombus (blood clot). Another example of a medical challenge to be addressed is obesity, which is one of the major health problems in developed countries. In most cases, overeating is the key problem, which can be circumvented by methods for curbing appetite. One solution may be biodegradable intragastric implants that inflate after an approximate predetermined time and provide the patient with a feeling of satiety after only a small amount of food has been eaten[61,62].

Shape-memory foams have been proposed as a measuring device to survey the shape of a human ear canal, so a hearing aid can be fitted properly[63]. The material is a commercially available polyurethane foam with a T_g switching transition. The foam shows full recovery after 83% compression. Another application of shape-memory polymers is in stents for the prevention of strokes[64]. Here, coils of a composite

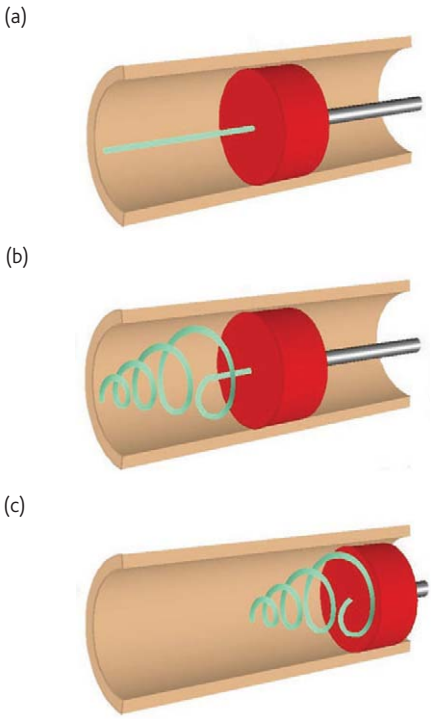

Fig. 8 Depiction of removal of a clot in a blood vessel using the laser-activated shape-memory polymer microactuator coupled to an optical fiber. (a) In its temporary straight rod form, the microactuator is delivered through a catheter distal to the blood clot. (b) The microactuator is then transformed into its permanent corkscrew form by laser heating. (c) The deployed microactuator is retracted to capture the thrombus. (Reprinted with permission from[40]. © 2005 The Optical Society of America.)

consisting of tantal and a polyetherurethane ($T_{trans} = T_g$; T_g = 33°C) have been studied. Tantal is needed as a radio-opaque filler for diagnostic detection. The filling does not affect the shape-recovery behavior but lowers T_g and the maximum recovery stress.

When polyurethane-based shape-memory polymers are used *in vivo*, biocompatibility and cytotoxicity have to be considered. In an *in vivo* study, commercially available aromatic shape-memory polyetherurethanes show similar biocompatibility and cytotoxicity compared with non-shape-memory polyurethanes[65]. Furthermore, it has been demonstrated that cell adhesion and cell growth can be promoted by protein coating, and cell platelet adhesion and reactivity is low.

Biodegradable shape-memory polymers

As well as responding to different stimulations, biodegradability would be beneficial for many medical applications[60]. The combination of shape-memory capability and biodegradability is an example of multifunctionality in a material[66]. This type of multifunctionality is especially advantageous for medical devices used for minimally invasive surgery. The polymers allow the insertion of bulky implants in a compressed shape into the human body through a small incision. When stimulated within the body, they turn into their application-relevant shape. Another example is a biodegradable shape-memory polymer as an intelligent suture for wound closure[7]. Upon actuation of the shape-memory effect, the material is able to apply a defined stress to the wound lips (Fig. 9). In both applications, removal of the implant in follow-up surgery is not necessary, as the implant degrades within a predefined time interval.

Biodegradability of shape-memory polymers can be realized by the introduction of weak, hydrolyzable bonds that cleave under physiological conditions. Generally, biodegradable polymers can be classified into surface- and bulk-eroding polymers[67]. While the first class shows a linear degradation characteristic, the latter shows nonlinear degradation. When diffusion of water into the polymer sample and the reactivity of the polymer functional groups are taken into account, the degradation type can be predicted[68]. Table 1 gives an overview of degradable shape-memory polymers for potential biomedical applications.

When biodegradable polymers are used in medical devices, the biocompatibility of the solid polymer and its degradation products have to be considered[69]. Additionally, medical applications require thorough sterilization of the materials[70]. Ethylene oxide (EO) and low-temperature plasma (LTP) sterilization are widely accepted low-temperature sterilization techniques for polymeric materials. When the influence of EO and LTP sterilization on an AB-type shape-memory polymer network based on poly(ε-caprolactone) dimethacrylate and n-butyl acrylate was investigated[71], statistically significant differences in the cell lysis in *in vitro* cell-screening tests could be detected[72]. In contrast, when chorioallantoic membrane tests (CAM test) are used as *in vivo* tests, no adverse effects on the angiogenesis (the growing of blood vessels) could be determined[72]. In these tests, a fertilized chicken egg is partly peeled and the polymer sample is placed on the outer skin of the egg in the shell-free area. Afterwards, the egg is incubated further. The differences between the *in vitro* and *in vivo* results have been attributed to EO remaining in the polymer material, Si particles from the EO sterilization, or surface oxidation during LTP sterilization. It is concluded that the polymer does not harm the surrounding tissue but appropriate choice of sterilization technique is important. This positive result was verified when the material was subcutaneously implanted in male NMRI (Naval Medical Research Institute) mice: a remarkable integration in the soft tissue coinciding with an early appearance of blood vessel formation was found[73]. This is notable because NMRI mice are lacking in thymus and are therefore especially sensitive to infections. In an animal model, the stability and integration into the adjacent tissue was examined[74]. No gas leakage after gas insufflation could be detected, and fast and unfavorable degradation of the polymer did not occur. A tight connection between the polymer and the adjacent stomach was found, resulting in adequate mechanical stability under the extreme pathophysical conditions of the stomach milieu.

Covalently cross-linked shape-memory polymers with $T_{trans} = T_g$ have been obtained in a polyaddition reaction of telechelic oligomers bearing several hydroxyl groups with diisocyanates[75]. An isomeric mixture of 1,6-diisocyanato-2,2,4-trimethylhexane and 1,6-diisocyanato-2,4,4-trimethylhexane was used to couple star-shaped oligoesters of *rac*-dilactide and diglycolide. As in aliphatic copolyesters

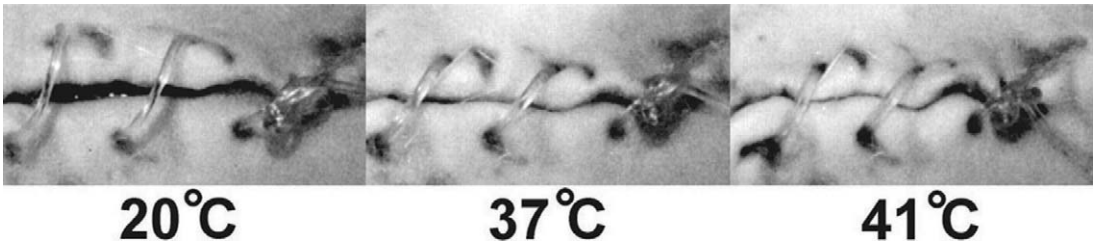

Fig. 9 Degradable shape-memory suture for wound closure. The photo series from an animal experiment shows (left to right) the shrinkage of the fiber while temperature increases. (Adapted and reprinted with permission from[7]. © 2002 American Association for the Advancement of Science.)

Table 1 Biodegradable shape-memory polymers.

Polymer	Shape-memory properties	Degradation properties 50%/complete	Biocompatibility *in vitro*	Biocompatibility *in vivo*
Poly(ε-caprolactone) dimethacrylate and *n*-butyl acrylate[71,72]	Third cycle R_f = 93-98% R_r ~ 95%	Phosphate buffer solution (pH 7.4; 37°C) No mass loss after 140 days	Statistically significant differences in cell lysis depending on sterilization technique	CAM test No adverse effects on angiogenesis
Star-shaped oligoesters of *rac*-dilactide and diglycolide[75]	Fifth cycle $R_f \geq 99\%$ $R_r \leq 97\%$	Aqueous buffer solution (pH 7; 37°C) 80 days/150 days	No data shown	No data shown
Multiblock copolyesters from poly(ε-caprolactone) and PEG, and chain extender based on CA groups[76]	Third cycle[a] R_f = 100% R_r = 88%	Phosphate buffer solution[a] (pH 7.2, 37°C) 5% after 25 days/ -	No data shown	No data shown
Oligo(ε-caprolactone) diols, oligo (*p*-dioxanone) diols, and diisocyanate[7,77,78]	Third cycle R_f = 98-99.5% R_r = 98-99%	Aqueous buffer solution[b] (pH 7; 37°C) 270 days/ -	No statistical difference on the activity of matrix metalloproteinases (MMPs) and tissue inhibitors of MMPs (TIMPS)[c]	CAM test[d] No avascular zones and/ or free capillaries
Multiblock copolymers containing poly(L-lactide) and poly[glycolide-*co*-(ε-caprolactone)]-segments[79]	Third cycle R_f ~ 99.0% R_r ~ 99.6%	Phosphate buffer solution (pH 7.4; 37°C) 154 days/ -	No data shown	No data shown

[a] *75 wt.% poly(ε-caprolactone) (M_n = 3000 gmol^{-1}), 25 wt.% poly(ethylene glycol) (M_n = 3000 gmol^{-1}), total M_n = 28 700 gmol^{-1}, gel content 57%*
[b] *42 wt.% oligo(p-dioxanone)*
[c] *Epithelial cell cultures of the upper aerodigestive tract seeded on a multiblock copolymer material 38 wt.% poly(p-dioxanone) and 56 wt.% poly(ε-caprolactone)*
[d] *38 wt.% poly(p-dioxanone) and 56 wt.% poly(ε-caprolactone)*

from diglycolide and dilactide, bulk erosion can be observed for this type of polymer. Covalently cross-linked biodegradable polymer networks with $T_{trans} = T_m$ were realized in multiblock copolyesters from poly(ε-caprolactone) and PEG and a chain extender based on CA groups[76]. Irradiation with light of suitable wavelengths (λ > 280 nm) results in [2 + 2] cycloaddition reaction of the CA moieties and forms the covalent cross-links. Here, the degradation properties can be controlled by the cross-link density, which is controlled by the irradiation time. Additionally, after an induction period, weight loss per day increases linearly with increasing PEG content.

Biodegradability has also been realized in thermoplastic shape-memory polymers consisting of linear block copolymers of oligo(ε-caprolactone)diols and oligo(*p*-dioxanone)diols, and using diisocyanate as a junction unit[7]. Here, oligo(ε-caprolactone) acts as crystallizable switching segment, while the phase related to T_{perm} is formed by crystalline oligo(*p*-dioxanone) segments. The multiblock copolymers display a linear mass loss *in vitro*, resulting in continuous release of degradation products. In *in vitro* cell seeding tests, no statistical difference could be determined between the shape-memory polymer sample and a polystyrene control sample[77]. This positive result has also been demonstrated in CAM tests[78].

Another example of a potentially biodegradable shape-memory polymer is a multiblock copolymer containing poly(L-lactide) and poly[glycolide-*co*-(ε-caprolactone)]-segments[79]. Here, degradability of the switching segment is increased by incorporation of easily hydrolyzable ester bonds with the drawback of nonlinear erosion. The polymer's biocompatibility has not been shown yet.

Conclusion and outlook

The field of actively moving polymers – polymers that are able to perform movements by themselves – is progressing rapidly[9]. Shape-memory polymers play a key role within this field. Fundamental shape-memory research is focusing on the implementation of stimuli other than heat to actuate shape-memory polymers, or to actuate them remotely. First examples include the light-induced stimulation of shape-memory polymers or the use of alternating magnetic fields

for remote actuation. It is assumed that these methods of stimulation will open up new fields of application. An important application area for shape-memory polymers is in active medical devices and implants[60], and initial demonstrations have been presented[39,40]. The application requirements can be complex in this area. Therefore, a trend toward the development of multifunctional materials can be seen[66]. Furthermore, there is a strong demand for actively moving materials able to perform complex movements. These requirements could be fulfilled by materials that are able to perform two or more predetermined shifts[80]. mt

REFERENCES

1. Hu, J., *et al., J. Dong Hua University Engl. Ed.* (2002) **19**, 89
2. Mondal, S., and Hu, J. L., *Indian J. Fibre Textile Res.* (2006) **31**, 66
3. Charlesby, A., *Atomic Radiation and Polymers*, Pergamon Press, New York, (1960), 198
4. Campbell, D., *et al.,* Elastic Memory Composite Material: An Enabling Technology For Future Furable Space Structures. In *46th AIAA/ASME/ASCE/AHS/ASC Structures, Structural Dynamics, and Materials Conference,* Austin, Texas, 2005
5. Hussein, H., and Harrison, D., Investigation into the use of engineering polymers as acutators to produce 'automatic disassembly' of electronic products. In *Design and Manufacture for Sustainable Development 2004,* Bhamra, T., and Hon, B., (eds.), Wiley-VCH, Weinheim, (2004)
6. Wache, H. M., *et al., J. Mater. Sci.: Mater. Med.* (2003) **14**, 109
7. Lendlein, A., and Langer, R., *Science* (2002) **296**, 1673
8. Metcalfe, A., *et al., Biomaterials* (2003) **24**, 491
9. Behl, M., and Lendlein, A., *Soft Matter* (2007) **3**, 58
10. Hornbogen, E., *Adv. Eng. Mater.* (2006) **8**, 101
11. Lendlein, A., and Kelch, S., *Angew. Chem. Int. Ed.* (2002) **41**, 2034
12. Lendlein, A., *et al.,* Shape-Memory Polymers. In *Encyclopedia of Materials: Science and Technology*, Buschow, K. H. J., *et al.,* (eds.), Elsevier, New York (2005)
13. Jiang, H. Y., *et al., Adv. Mater.* (2006) **18**, 1471
14. Morshedian, J., *et al., Macromol. Theory Simul.* (2005) **14**, 428
15. Liu, Y. P., *et al., Int. J. Plasticity* (2006) **22**, 279
16. Diani, J., *et al., Polym. Eng. Sci.* (2006) **46**, 486
17. Barot, G., and Rao, I. J., *Z. Angew. Math. Phys.* (2006) **57**, 652
18. Kim, B. K., *et al., Polymer* (1996) **37**, 5781
19. Li, F. K., *et al., J. Appl. Polym. Sci.* (1996) **62**, 631
20. Ma, Z. L., *et al., J. Appl. Polym. Sci.* (1997) **63**, 1511
21. Jeong, H. M., *et al., J. Mater. Sci.* (2000) **35**, 279
22. Jeong, H. M., *et al., Polymer* (2000) **41**, 1849
23. Ni, X., and Sun, X., *J. Appl. Polym. Sci.* (2006) **100**, 879
24. Cho, J. W., *et al., J. Appl. Polym. Sci.* (2004) **93**, 2410
25. Booth, C. J., *et al., Polymer* (2006) **47**, 6398
26. Perez-Foullerat, D., *et al., Macromol. Chem. Phys.* (2004) **205**, 374
27. Kleinhans, G., *et al., Kunststoffe* (1984) **74**, 445
28. Kleinhans, G., and Heidenhain, F., *Kunststoffe* (1986) **76**, 1069
29. Zhu, G., *et al., J. Appl. Polym. Sci.* (2003) **90**, 1589
30. Zhu, G. M., *et al., Radiat. Phys. Chem.* (2006) **75**, 443
31. Li, F. K., *et al., J. Appl. Polym. Sci.* (1999) **71**, 1063
32. Liu, C. D., *et al., Macromolecules* (2002) **35**, 9868
33. Li, F. K., and Larock, R. C., *J. Appl. Polym. Sci.* (2002) **84**, 1533
34. Kagami, Y., *et al., Macromol. Rapid Commun.* (1996) **17**, 539
35. Goethals, E. J., *et al., Macromol. Symp.* (1998) **132**, 57
36. Reyntjens, W. G., *et al., Macromol. Rapid Commun.* (1999) **20**, 251
37. Lee, S. H., *et al., Smart Mater. Struct.* (2004) **13**, 1345
38. Rousseau, I. A., and Mather, P. T., *J. Am. Chem. Soc.* (2003) **125**, 15300
39. Maitland, D. J., *et al., Lasers Surg. Med.* (2002) **30**, 1
40. Small, W., *et al., Opt. Express* (2005) **13**, 8204
41. Liu, C. D., and Mather, P. T., *ANTEC Proc.* (2003), 1962
42. Biercuk, M. J., *et al., Appl. Phys. Lett.* (2002) **80**, 2767
43. Li, F. K., *et al., J. Appl. Polym. Sci.* (2000) **75**, 68
44. Liang, C., *et al., J. Intelligent Mater. Systems Struct.* (1997) **8**, 380
45. Gall, K., *et al., J. Intelligent Mater. Systems Struct.* (2000) **11**, 877
46. Ash, B. J., *et al.,* Investigation into the thermal mechanical behavior of PMMA/alumina nanocomposites. In *Filled and Nanocomposite Polymer Materials*. Materials Research Society, Boston, (2001) KK2.10.1
47. Bhattacharya, S. K., and Tummala, R. R., *J. Electron. Packaging* (2002) **124**, 1
48. Koerner, H., *et al., Nat. Mater.* (2004) **3**, 115
49. Cho, J. W., *et al., Macromol. Rapid Commun.* (2005) **26**, 412
50. Mohr, R., *et al., Proc. Natl. Acad. Sci. USA* (2006) **103**, 3540
51. Buckley, P. R., *et al., IEEE Trans. Biomed. Eng.* (2006) **53**, 2075
52. Yang, B., *et al., Smart Mater. Struct.* (2004) **13**, 191
53. Huang, W. M., *et al., Appl. Phys. Lett.* (2005) **86**, 114105
54. Yang, B., *et al., Polymer* (2006) **47**, 1348
55. Yang, B., *et al., Scripta Mater.* (2005) **53**, 105
56. Jung, Y. C., *et al., J. Macromol. Sci., Phys.* (2006) **45**, 453
57. Lendlein, A., *et al., Nature* (2005) **434**, 879
58. Yu, Y. L., and Ikeda, T., *Macromol. Chem. Phys.* (2005) **206**, 1705
59. Langer, R., and Tirrell, D. A., *Nature* (2004) **428**, 487
60. El Feninat, F., *et al., Adv. Eng. Mater.* (2002) **4**, 91
61. Lendlein, A., and Langer, R. S., Self-expanding device for the gastrointestinal or urogenital area. WO 2004073690 A1, 2004
62. Marco, D., Biodegradable self-inflating intragastric implants for curbing appetite. WO 2006092789 A2, 2006
63. Huang, W. M., *et al., J. Intelligent Mater. Systems Struct.* (2006) **17**, 753
64. Hampikian, J. M., *et al., Mater. Sci. Eng. C* (2006) **26**, 1373
65. Farè, S., *et al., J. Biomed. Mater. Res. A* (2005) **73A**, 1
66. Lendlein, A., and Kelch, S., Degradable, multifunctional polymeric biomaterials with shape-memory. In *Functionally Graded Materials VIII*, Van der Biest, O., *et al.*, (eds.), Tech Trans Publications, Zurich, Switzerland (2005), **492-493**, 219
67. Tamada, J. A., and Langer, R. *Proc. Natl. Acad. Sci. USA* (1993) **90**, 552
68. von Burkersroda, F., *et al., Biomaterials* (2002) **23**, 4221
69. Zange, R., *et al., J. Controlled Release* (1998) **56**, 249
70. Wallhäuser, K., *Praxis der sterilization-desinfektion-konservierung*. 5th Edition, Georg Thieme Verlag, Stuttgart, Germany (1995)
71. Lendlein, A., *et al., Proc. Natl. Acad. Sci. USA* (2001) **98**, 842
72. Rickert, D., *et al., J. Biomed. Mater. Res. B* (2003) **67B**, 722
73. Binzen, E., *et al., Clin. Hemorheol. Microcirc.* (2004) **30**, 283
74. Rickert, D., *et al., Biomed. Technik* (2006) **51**, 116
75. Alteheld, A., *et al., Angew. Chem. Int. Ed.* (2005) **44**, 1188
76. Nagata, M., and Kitazima, I., *Colloid Polym. Sci.* (2006) **284**, 380
77. Rickert, D., *et al., Clin. Hemorheol. Microcirc.* (2005) **32**, 117
78. Rickert, D., *et al., Clin. Hemorheol. Microcirc.* (2003) **28**, 175
79. Min, C. C., *et al., Polym. Adv. Technol.* (2005) **16**, 608
80. Bellin, I., *et al., Proc. Natl. Acad. Sci. USA* (2006) **103**, 18043
81. Lendlein, A., *et al., Kunststoffe Int.* (2006) **96**, 54